Single-Photon Excitation of Surface Plasmon Polaritons

M. S. Tame,[1] C. Lee,[2] J. Lee,[2,3] D. Ballester,[1] M. Paternostro,[1] A. V. Zayats,[4] and M. S. Kim[1]

[1]*School of Mathematics and Physics, Queen's University, Belfast BT7 1NN, United Kingdom*
[2]*Department of Physics, Hanyang University, Seoul 133-791, Korea*
[3]*Quantum Photonic Science Research Center, Hanyang University, Seoul 133-791, Korea*
[4]*Centre for Nanostructured Media, IRCEP, Queen's University, Belfast BT7 1NN, United Kingdom*
(Received 21 April 2008; published 7 November 2008)

We provide the quantum-mechanical description of the excitation of surface plasmon polaritons on metal surfaces by single photons. An attenuated-reflection setup is described for the quantum excitation process in which we find remarkably efficient photon-to-surface plasmon wave-packet transfer. Using a fully quantized treatment of the fields, we introduce the Hamiltonian for their interaction and study the quantum statistics during transfer with and without losses in the metal.

DOI: 10.1103/PhysRevLett.101.190504 PACS numbers: 03.67.−a, 03.70.+k, 42.50.Dv, 42.50.Ex

The emerging field of plasmonics [1] is experiencing a considerable increase in interest from researchers in many areas of the physical sciences [2]. Plasmonic-based nanophotonic devices, in particular, have begun to attract keen interest from the quantum optics community for their use in quantum-information processing [3–6]. In order to unlock the potential that plasmonics at the quantum level can offer, a clear understanding of the interplay between single photons and surface plasmon polaritons (SPPs) is of fundamental importance. Recent studies have focused on various systems where SPPs and photons interact [4–6]. However, a major obstacle has been the low transfer efficiencies found at the single-photon level [4,5], thus a complete quantum description of an efficient transfer process is highly desirable. With an extensive understanding of photon-SPP coupling in the quantum regime, we can expect to open up an array of new applications in quantum-information processing, based on linear and nonlinear plasmonic effects facilitated by strong electromagnetic field confinement [5,7].

In this Letter we provide the first *quantum* description of the coupling between single photons and SPPs in a versatile attenuated-reflection (ATR) setup previously used only for *classical* SPP generation [8,9]. This is distinct from earlier work, such as couplings at rough surfaces [10], requiring an entirely different approach. The Hamiltonian that we introduce is based on a fully quantized treatment of both photon and SPP field modes and applies to a wide range of ATR parameters. We find that remarkably high *quantum efficiencies* can be reached for photon-to-SPP transfer. We then establish the extent to which the excited SPPs preserve the quantum statistics of the photons as they travel on realistic metal surfaces. Our work provides significant insights into the physics of photon-SPP coupling at the quantum level. The methods developed are well suited to other coupling geometries.

SPPs are highly confined, nonradiative electromagnetic excitations associated with electron charge density waves propagating along a dielectric-metal interface. In Fig. 1(a) we show the ATR setup utilized for single-photon excitation of SPPs. At various points we will introduce the metal as silver only to illustrate our main results; the theory developed here fits a far more general setting. For SPP excitations, due to the collective nature of the electron charge density waves, a macroscopic picture of the resulting electromagnetic field is appropriate [10]. Upon quantization, SPPs therefore correspond to bosonic modes. The quantized vector potential in the continuum limit for SPPs propagating along an air-metal interface at $z = 0$ in the $\hat{\mathbf{x}}$ direction, as shown on the right-hand side of Fig. 1(a), is given by [10,11] $\hat{\mathbf{A}}_{\rm SPP}(\mathbf{r}, t) \propto \int_0^\infty d\omega[\mathcal{N}(\omega)L]^{-1/2} \times [\boldsymbol{\phi}(\mathbf{r}, \omega)e^{-i\omega t}\hat{b}(\omega) + \text{H.c.}]$. The dispersion relation is $\omega^2 = c^2k^2(\epsilon_m + 1)/\epsilon_m$ with ϵ_m the permittivity of the metal, $\mathcal{N}(\omega)$ is a frequency dependent normalization [10], and L is the *profile width* [11]. The $\hat{b}(\omega)$'s [$\hat{b}^\dagger(\omega)$'s] correspond to annihilation [creation] operators which obey commutation relations $[\hat{b}(\omega), \hat{b}^\dagger(\omega')] = \delta(\omega - \omega')$. The mode functions are given by $\boldsymbol{\phi}(\mathbf{r}, \omega) = [(i\hat{\mathbf{x}} - k\hat{\mathbf{z}}/\nu)e^{-\nu z}\vartheta(z) + (i\hat{\mathbf{x}} + k\hat{\mathbf{z}}/\nu_0)e^{\nu_0 z}\vartheta(-z)]e^{i\mathbf{k}\cdot\mathbf{r}}$, where the wave vector $\mathbf{k} = k\hat{\mathbf{x}}$, $\vartheta(z)$ is the Heaviside step function, and the decay of the SPP into the metal (air) is parametrized by $\nu^2 = k^2 - \epsilon_m\omega^2/c^2$ ($\nu_0^2 = k^2 - \omega^2/c^2$). For photons propagating in air in the $\hat{\mathbf{k}}'$ direction [$\hat{\mathbf{k}}' = (\sin\theta)\hat{\mathbf{x}} + (\cos\theta)\hat{\mathbf{z}}$, as shown in the left-hand side of Fig. 1(a)], we have [11] $\hat{A}_P(\mathbf{r}, t) \propto \int_0^\infty d\omega(\omega A)^{-1/2}[e^{ik'(\hat{\mathbf{k}}'\cdot\mathbf{r})}e^{-i\omega t}\hat{a}(\omega) + \text{H.c.}]$. The dispersion relation is $\omega = ck'$, A is the beam cross section, and $[\hat{a}(\omega), \hat{a}^\dagger(\omega')] = \delta(\omega - \omega')$. Here, the SPPs and photons are transverse magnetic modes. At the single-photon level only small intensities of the photon field are involved and any nonlinear terms in the photon-SPP coupling can be sufficiently neglected [12]. We are thus led to the following natural linear coupling Hamiltonian for the entire system shown in Fig. 1(a):

$$\hat{\mathcal{H}}_S = \int_0^\infty d\omega\hbar\omega\hat{a}^\dagger(\omega)\hat{a}(\omega) + \int_0^\infty d\omega\hbar\omega\hat{b}^\dagger(\omega)\hat{b}(\omega) + i\hbar\int_0^\infty d\omega[g(\omega)\hat{a}^\dagger(\omega)\hat{b}(\omega) - g^*(\omega)\hat{b}^\dagger(\omega)\hat{a}(\omega)]. \quad (1)$$

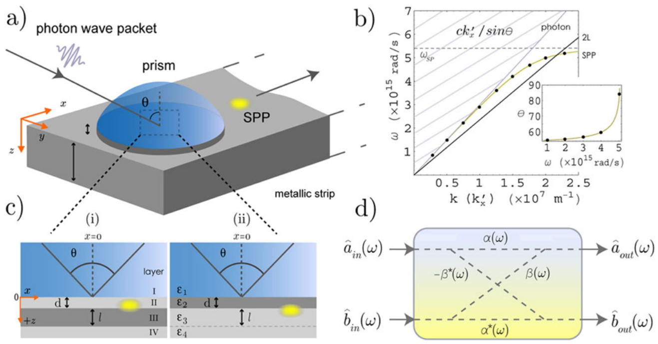

FIG. 1 (color online). Single-photon excitation of SPPs using attenuated reflection. (a) A photon wave packet is injected into the system at a specific angle θ, with a prism mediating an interaction between the photon and SPP modes. The minimum prism size is diffraction-limited. (b) Dispersion relations for the photon (shaded region) and SPP (curve). The prism enables mode matching. (c) Two ATR excitation geometries: (i) Otto and (ii) Kretschmann-Raether; see text for details. (d) Transfer process for the photon and SPP mode operators.

The first and second terms are the photon and SPP fields' free energy, respectively. The last term, which we denote as $\hat{\mathcal{H}}_{\rm int}$, describes interactions between the two fields, where the coupling $g(\omega)$ is a function of the system parameters for a given ATR geometry. In Fig. 1(b) we show the dispersion relations for SPPs and photons. As an example, we choose $\epsilon_m = 1 - \omega_p^2/\omega^2 + \delta\epsilon_m^r$, where $\omega_p = 1.402 \times 10^{16}$ rad/s is the plasma frequency for silver and $\delta\epsilon_m^r = 29\omega^2/\omega_p^2$ is a background correction term [13]. Neglecting Ohmic losses, over the ω range of the SPP modes, k produces a curve which approaches the surface plasma frequency $\omega_{\rm sp}$, where $\epsilon_m = -1$. On the other hand, the $\hat{\mathbf{x}}$ component of $\mathbf{k}'$ for photons in air incident at angle θ covers the shaded region of Fig. 1(b). Two ATR geometries that can provide the necessary mode matching for coupling photons to SPPs are shown in Fig. 1(c), denoted as (i) Otto (O) [8] and (ii) Kretschmann-Raether (KR) [9]. Both consist of a prism in layer I with permittivity ϵ_1. The O (KR) geometry has air in layers II and IV (III and IV) with $\epsilon_2 = \epsilon_4 = 1$ ($\epsilon_3 = \epsilon_4 = 1$) and metal in layer III (II) with $\epsilon_3 = \epsilon_m$ ($\epsilon_2 = \epsilon_m$). In both, SPPs are excited on the II/III interface, with $z \to z - d$ in $\boldsymbol{\phi}(\mathbf{r}, \omega)$. For the KR geometry, $\nu \leftrightarrow \nu_0$. The thickness l is assumed to be far larger than the decay of the SPP into the metal (air), i.e., $l \gg \nu^{-1}$ (ν_0^{-1}), making the effects of layer IV negligible.

With the ATR setup introduced, we can now formulate the photon-SPP coupling model of Eq. (1). For each ω in both geometries the coupling can be described by a transfer matrix $\mathcal{T}(\omega)$ in the Heisenberg picture [14] as

$$\begin{pmatrix} \hat{a}_{\rm out}(\omega) \\ \hat{b}_{\rm out}(\omega) \end{pmatrix} = \begin{pmatrix} \alpha(\omega) & \beta(\omega) \\ -\beta^*(\omega) & \alpha^*(\omega) \end{pmatrix} \begin{pmatrix} \hat{a}_{\rm in}(\omega) \\ \hat{b}_{\rm in}(\omega) \end{pmatrix}. \quad (2)$$

The transfer process is depicted in Fig. 1(d), where the commutation relations of the quantum operators $\hat{a}(\omega)$ and $\hat{b}(\omega)$ define the structure of $\mathcal{T}(\omega)$, while its coefficients $[|\alpha(\omega)|^2 + |\beta(\omega)|^2 = 1, \ \forall\ \omega]$ are determined from the overlap of system mode functions. By solving Maxwell's equations across the first three layers shown in Fig. 1(c), one finds the mode functions of the field in layers II and III: $\boldsymbol{\psi}(\mathbf{r}, \omega) = \{[(\varphi_1 e^{-\gamma_2 z} + \varphi_2 e^{\gamma_2 z})\hat{\mathbf{x}} + (\varphi_3 e^{-\gamma_2 z} + \varphi_4 e^{\gamma_2 z})\hat{\mathbf{z}}]\vartheta(z)\vartheta(d - z) + (\varphi_5 e^{-\gamma_3 z}\hat{\mathbf{x}} + \varphi_6 e^{-\gamma_3 z}\hat{\mathbf{z}})\vartheta(z - d)\}e^{i\kappa x}$. Here, the φ_i's are constants related by boundary conditions at the interfaces, $\gamma_i = (\kappa^2 - \epsilon_i\omega^2/c^2)^{1/2}$, and the dispersion relation $\kappa = \sqrt{\epsilon_1}(\omega/c)\sin\theta$. The O (KR) geometry has $\epsilon_2 = 1$ (ϵ_m) and $\epsilon_3 = \epsilon_m$ (1) with $\epsilon_m = 1 - \omega_p^2/(\omega^2 + i\omega\Gamma) + \delta\epsilon_m$, which now includes a damping factor Γ for the metal and a complex correction term $\delta\epsilon_m$ [13]. The complete mode functions for the three-layer ($3L$) system are $\boldsymbol{\Psi}(\mathbf{r}, \omega) = r\tilde{\boldsymbol{\psi}}(\mathbf{r}, \omega)\vartheta(-z) + \tau\boldsymbol{\psi}(\mathbf{r}, \omega)\vartheta(z)$ where r and τ ($|r|^2 + |\tau|^2 = 1$) are obtained from Fresnel's relations at the boundaries. However, the $\tilde{\boldsymbol{\psi}}(\mathbf{r}, \omega)$ are not involved in the coupling due to mode matching; they always have a real component of their wave vector in $\hat{\mathbf{z}}$. On the other hand, mode matching can be satisfied between the two-layer ($2L$) mode functions $\boldsymbol{\psi}(\mathbf{r}, \omega)$ and the SPP mode functions by fixing the angle θ correctly. For instance, by setting $\kappa = k$ the dispersion lines cross at $\theta = \sin^{-1}\{\epsilon_m/[\epsilon_1(1 + \epsilon_m)]\}^{1/2}$ in both geometries. In Fig. 1(b) we show this for a particular angle $\theta = 85°$ ($2L$ line). The inset shows that mode matching over the entire range of ω can be achieved, for example, using a prism with $\epsilon_1 = 1.51$ and silver with $\Gamma = 6.25 \times 10^{13}$ rad/s and $\delta\epsilon_m = \delta\epsilon_m^r + i\delta\epsilon_m^i$, where $\delta\epsilon_m^i = 0.22$ [13]. This range is important for excitation with a photon wave packet of finite width, as we show later, and is not possible in other excitation schemes such as the grating-type coupler.

In Fig. 1(d) the $\hat{b}_{\rm in/out}(\omega)$ operators are associated with the in/out SPP mode functions $\boldsymbol{\phi}(\mathbf{r}, \omega)$ $[\hat{b}_{\rm in}(\omega) = \hat{b}(\omega)]$ and $\hat{a}_{\rm in/out}(\omega)$ with the in/out $3L$ mode functions $\boldsymbol{\Psi}(\mathbf{r}, \omega)$. For negligible loss on entry into the prism medium, we can assume the operator relation $\hat{a}_{\rm in}(\omega) = \hat{a}(\omega)$. We then have $\beta^*(\omega) = -\tau\{\delta(\omega - \omega')\delta(k - \kappa) \times \int dz[\mathcal{N}_1^{-1/2}(\omega)\boldsymbol{\phi}(\mathbf{r}, \omega)]^* \cdot [\mathcal{N}_2^{-1/2}(\omega')\boldsymbol{\psi}(\mathbf{r}, \omega')]\}$ [15]. Several factors permit the use of the mode overlap in the value of $\beta^*(\omega)$. First, we assume that the SPP modes experience negligible damping during the excitation process, ${\rm Im}(\epsilon_m) \approx 0$, imposing damping effects subsequently as the SPP propagates. Second, the SPP is assumed to exit the prism region on a time scale such that mode-matching conditions are broken almost immediately after excitation. This can be achieved by adjusting the excitation point [16]. Third, as the SPP mode functions exist in the region $z \in (-\infty, \infty)$, d must be chosen such that their decay into the prism is negligible, allowing it to be neglected from their definitions. To check an acceptable range of d we define a *penetration factor* $\mathcal{P} = 2/\nu_0 d$ ($2/\nu d$) for the O (KR) geometry and consider the SPP modes as good approximations for $\mathcal{P} \leq 1$, where $|\boldsymbol{\phi}(\mathbf{r}, \omega)|^2$ at $z = 0$ is less than 2% its maximum value. In Figs. 2(a) and 2(b) we use the example of silver to show $\mathcal{P}$ over a range of ω and d for the two ATR geometries.

With the above considerations, we can now determine the coupling $g(\omega)$. In order to connect $\beta^*(\omega)$ and $g(\omega)$, we set $\alpha = \cos\Theta$ and $\beta = e^{i\Phi}\sin\Theta$ ($\Theta \in [0, \pi/2]$, $\Phi \in [0, 2\pi]$) for each ω and parameter set $\{d, \epsilon_i, \theta\}$ for a given geometry. The corresponding Hamiltonian in the Schrödinger picture is $\hat{\mathcal{H}}_{\rm int}$ from Eq. (1) with $g(\omega) = e^{i\Phi(\omega)}\Theta(\omega)$ [14]. In Figs. 2(c) and 2(d) we use silver to plot a rescaled coupling, $|\tilde{g}(\omega)| = \frac{2}{\pi}|g(\omega)|$, for the two ATR geometries, such that $|\tilde{g}(\omega)| = 1$ (0) corresponds to a unit (zero) transfer probability of a photon to a SPP. Figures 2(a) and 2(b) show that the optimal $|\tilde{g}(\omega)|$ for both geometries satisfy $\mathcal{P} \lesssim 1$. In Figs. 2(e) and 2(f) we plot these optimal values and the value of d at which they occur. The optimal $|\tilde{g}(\omega)|$ in both geometries rises for increasing ω, reaching an apex, then drops sharply as ω tends toward $\omega_{\rm sp}$. This behavior is due to a dominance of the value for τ in $\beta^*(\omega)$ at large ω, which decreases rapidly due to boundary conditions and the large θ required for mode matching. Such excellent coupling values have been found *classically* [8,9], however, this is the first time a rigorous *quantum-mechanical* treatment has been achieved, making it possible for us to determine correctly the quantum efficiency of single-photon excitation. The coupling $g(\omega)$ cannot be deduced from a classical model of the system.

Thus far we have focused on single modes of the system. However, it is important to consider the transfer of a photon wave packet, such as in an experiment, to a SPP wave-packet state. An n-photon wave-packet state is given by $|n_\xi\rangle = (n!)^{-1/2}(\hat{a}_\xi^\dagger)^n|0\rangle$, where $\hat{a}_\xi^\dagger = \int d\omega\xi(\omega)\hat{a}^\dagger(\omega)$ with $\int d\omega|\xi(\omega)|^2 = 1$ [11]. For simplicity we take a Gaussian profile $\xi(\omega)$ for a wave packet produced at time $t_0 = 0$ with bandwidth $\Delta\omega = 2\sigma\sqrt{2\log 2}$ and central frequency ω_0. We allow $\omega \in (-\infty, \infty)$ as $\Delta\omega \ll \omega$. For wave-packet transfer with negligible *deformation*, each ω must have approximately the same $g(\omega)$ and θ. This is satisfied given a small enough bandwidth with slowly varying $g(\omega)$ and θ. For example, using silver with $\Delta\lambda = 10$ nm, one finds that $\Delta\theta$ rises exponentially from 0.004° at 1×10^{15} rad/s to 14.61° at 5×10^{15} rad/s, which can be attributed to the dependence of θ on ω [see inset of Fig. 1(b)]. The couplings show a similar behavior, with $|\Delta g(\omega)| = 0.01$ for d optimizing $|g(\omega_0)|$ at 1×10^{15} rad/s, rising to $|\Delta g(\omega)| = 0.2$ (0.04) at 5×10^{15} rad/s for the O (KR) geometry. The large difference is due to the sharper drop in $|g(\omega)|$ for O at high ω. Significant wave-packet deformation can be avoided by operating at low ω, although at the expense of the coupling. In general, a narrow bandwidth will provide access to larger couplings with negligible deformation.

Finally we turn our attention to damping in the metal as the excited SPP propagates. For the coupling, the approximation $\mathrm{Im}(\epsilon_m) \approx 0$ was made for the excited SPP. However, as it travels, finite conductivity of the metal and

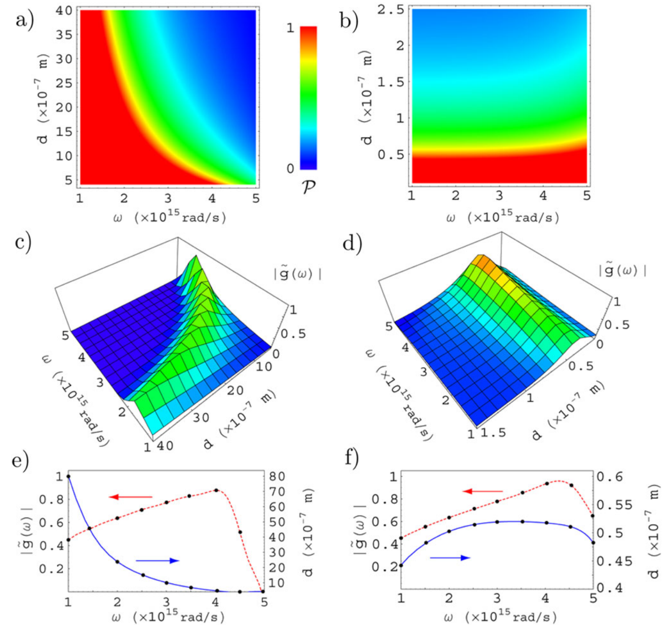

FIG. 2 (color online). Photon-SPP coupling: The left (right) column corresponds to the O (KR) geometry. (a) and (b) depict the penetration factor $\mathcal{P}$. (c) and (d) show the behavior of the coupling $|\tilde{g}(\omega)| = \frac{2}{\pi}|g(\omega)|$. The optimal values of $|\tilde{g}(\omega)|$ (dashed line) are displayed in (e) and (f) along with the values of d (solid line) at which they occur.

surface roughness result in heating and radiative losses, respectively [1]; for a reasonably smooth surface, thermal loss is the main source of damping. While a quantization of the decayed SPP modes can be performed, a mathematically equivalent and simpler model is the method of arrays shown in Fig. 3(a) [11]. Here we introduce a bath of field modes, described by operators $\hat{c}_i(\omega)$ $(i = 1, .., N)$ separated by Δx, interacting with the SPP wave packet as it propagates. In the limit $N \to \infty$ and $\Delta x \to 0$, the SPP operator becomes $\hat{b}^D_{\rm out}(\omega) = e^{iKx}\hat{b}_{\rm out}(\omega) + i\sqrt{2\kappa(\omega)}\int_0^x dx' e^{iK(x-x')}\hat{c}(\omega, x')$, with $\hat{c}_i(\omega) \to \sqrt{\Delta x}\hat{c}(\omega, x')$ and $\delta_{ij} \to \Delta x\delta(x' - x'')$. The array coefficients are chosen such that the bath modes induce a change in the SPP wave vector k matching that of the complex ϵ_m, i.e., $k \to K = (\omega/c)[\epsilon_m/(1 + \epsilon_m)]^{1/2} = k + i\kappa(\omega)$, where $2\kappa(\omega)$ is the loss per unit length of propagation. We then set the relations $\langle\hat{c}(\omega, x')\rangle = \langle\hat{c}^\dagger(\omega, x')\rangle = \langle\hat{c}^\dagger(\omega, x')\hat{c}(\omega, x'')\rangle = 0$ for the bath modes at room temperature and the frequencies considered [11]. We assume that the excited SPP wave packet with ω_0 has a narrow enough bandwidth such that $\kappa(\omega) \approx \kappa(\omega_0) = \kappa_0$ and $k \approx k(\omega_0) + (\omega - \omega_0)v_G^{-1}(\omega_0)$, with $v_G^{-1}(\omega_0) = \frac{\partial k(\omega)}{\partial \omega}|_{\omega=\omega_0}$. The flux of SPPs at point x along the metal surface is then simply $f_{\rm out}(t) = \langle\hat{b}^{D\dagger}_{\rm out}(t)\hat{b}^D_{\rm out}(t)\rangle = e^{-2\kappa_0 x}\langle\hat{b}^\dagger_{\rm out}(t_R)\hat{b}_{\rm out}(t_R)\rangle$, where $t_R = t - xv_G^{-1}(\omega_0)$. For an initial SPP wave packet with n excitations, $\langle\hat{b}^\dagger_{\rm out}(t_R)\hat{b}_{\rm out}(t_R)\rangle = n|\tilde{\xi}(t_R)|^2$. A detector with efficiency μ [11,17] operating for time period $[xv_G^{-1}(\omega_0) - 1/\sigma,\ xv_G^{-1}(\omega_0) + 1/\sigma]$ would measure a

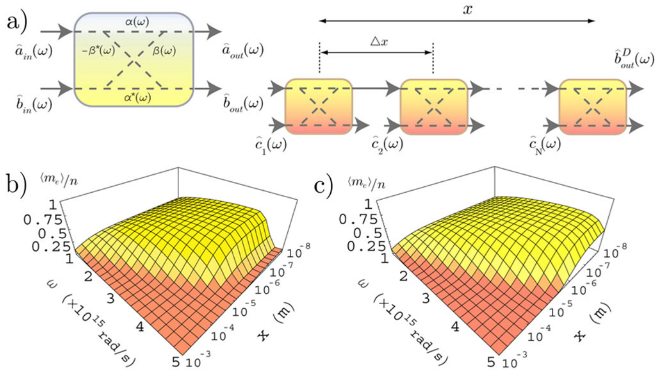

FIG. 3 (color online). Damping model for propagating SPPs. (a) Bath modes interact with the SPP mode as it travels along the metal. (b) and (c) show the normalized expected mean SPP count $\langle m_e \rangle / n$ at point x for an n photon-to-SPP wave-packet transfer via the O and KR geometries, respectively.

mean SPP count of $\langle m \rangle = \mu \int dt f_{\mathrm{out}}(t) = \mu n e^{-2\kappa_0 x}$. The photon-to-SPP transfer process must, however, be incorporated for determining the *expected* mean SPP count $\langle m_e \rangle$ from an incident n photon wave packet. The entire process is analogous to an inefficient detection problem [17] and we have $\langle m_e \rangle = \mu |\beta(\omega_0)|^2 n e^{-2\kappa_0 x}$. In Figs. 3(b) and 3(c) we show $\langle m_e \rangle / n$ for the ATR geometries, where $\mu = 0.65$ is chosen as an example of nonideal signal extraction using, e.g., a prism and photodetector. The detection of many identical excitations from a set rate of single photons would be required to determine $\langle m_e \rangle$.

While the quantum observable $\langle m_e \rangle$ matches well the behavior of its classical counterpart, the field intensity I [1], it is not sufficient in an experiment to show that the SPPs are quantum excitations. We now consider another observable, the zero time delay second-order quantum coherence function $g^{(2)}(0)$ [11] at a fixed position, defined as $g^{(2)}(0) = \langle : \hat{I}^2(t) : \rangle / \langle : \hat{I}(t) : \rangle^2$. Here, $\hat{I}$ is the intensity of the quantized field operator, :: denotes normal ordering, and the expectation value is taken over the *initial* state of the field. For a classical field $1 \leq g^{(2)}(0) \leq \infty$. On the other hand, for an incident n photon wave packet $g^{(2)}(0) = \langle m(m-1) \rangle / \langle m \rangle^2$, where $\langle m \rangle = n \int_t^{t+T} dt' |\tilde{\xi}(t')|^2$ and $\langle m(m-1) \rangle = n(n-1)[\int_t^{t+T} dt' |\tilde{\xi}(t')|^2]^2$, giving $g^{(2)}(0) = 1 - 1/n$. This always lies in the classically *forbidden* region $g^{(2)}(0) < 1$. The value of $g^{(2)}(0)$ for an excited SPP wave packet at point x can be found by recognizing that the photon-to-SPP transfer and SPP propagation stages constitute an array of lossy beam splitters [17]. At a beam splitter with loss coefficient $\eta^{1/2}$, the quantum observables $\langle m \rangle \to \eta \langle m \rangle$ and $\langle m(m-1) \rangle \to \eta^2 \langle m(m-1) \rangle$. Thus, the individual losses accumulated cancel, leaving $g^{(2)}(0)$ surprisingly unaffected. A Hanbury-Brown–Twiss-type experiment [18] could be used to measure $g^{(2)}(0)$.

We have provided the first quantum description of the photon-to-SPP transfer process for ATR excitation. Remarkably good quantum couplings over a wide range of frequencies were found. We also examined the extent to which the excited SPPs preserve quantum statistical properties. The techniques developed here provide key insights into the formulation of quantum descriptions for the photonic excitation of SPPs. This work can therefore be seen as an important starting point for future research into the design of new quantum plasmonic devices for applications based at the nanoscale, such as SPP-enhanced nonlinear photon interactions and SPP-assisted photonic quantum networking and processing.

We thank M. D. Lukin, S. Song, and S. K. Ozdemir for helpful discussions and acknowledge funding from EPSRC, QIPIRC, KRF (2005-041-C00197), and ESF.

[1] A. V. Zayats, I. I. Smolyaninov, and A. A. Maradudin, Phys. Rep. **408**, 131 (2005).
[2] W. L. Barnes, A. Dereux, and T. W. Ebbesen, Nature (London) **424**, 824 (2003).
[3] J. L. van Velsen, J. Tworzydlo, and C. W. J. Beenakker, Phys. Rev. A **68**, 043807 (2003); S. Fasel *et al.*, New J. Phys. **8**, 13 (2006).
[4] E. Altewischer, M. P. van Exter, and J. P. Woerdman, Nature (London) **418**, 304 (2002); E. Moreno *et al.*, Phys. Rev. Lett. **92**, 236801 (2004); S. Fasel *et al.*, Phys. Rev. Lett. **94**, 110501 (2005).
[5] D. E. Chang *et al.*, Phys. Rev. Lett. **97**, 053002 (2006); A. V. Akimov *et al.*, Nature (London) **450**, 402 (2007).
[6] D. E. Chang *et al.*, Nature Phys. **3**, 807 (2007).
[7] J. C. Quail, J. G. Rako, H. J. Simon, and R. T. Deck, Phys. Rev. Lett. **50**, 1987 (1983); I. I. Smolyaninov, A. V. Zayats, A. Gungor, and C. C. Davis, Phys. Rev. Lett. **88**, 187402 (2002); M. D. Lukin and A. Imamoglu, Nature (London) **413**, 273 (2001).
[8] A. Otto, Z. Phys. **216**, 398 (1968).
[9] E. Kretschmann and H. Raether, Z. Naturforsch. **23A**, 2135 (1968).
[10] J. M. Elson and R. H. Ritchie, Phys. Rev. B **4**, 4129 (1971).
[11] R. Loudon, *The Quantum Theory of Light* (Oxford University, Oxford, 2000), 3rd ed.
[12] H. J. Simon, D. E. Mitchell, and J. G. Watson, Phys. Rev. Lett. **33**, 1531 (1974).
[13] P. B. Johnson and R. W. Christy, Phys. Rev. B **6**, 4370 (1972).
[14] R. A. Campos, B. E. A. Saleh, and M. C. Teich, Phys. Rev. A **40**, 1371 (1989).
[15] The normalizations $\mathcal{N}_i$ are carried out over $z \in (-\infty, \infty)$.
[16] J. M. Montgomery and S. K. Gray, Phys. Rev. B **77**, 125407 (2008).
[17] H. P. Yuen and J. H. Shapiro, IEEE Trans. Inf. Theory **26**, 78 (1980).
[18] R. Hanbury-Brown and R. Q. Twiss, Nature (London) **177**, 27 (1956).